A Second Look at First Significant Digit Histogram Restoration

Matthias Kirchner and Sujoy Chakraborty
Department of Electrical and Computer Engineering
Binghamton University
Binghamton, NY 13902–6000
Email: {kirchner, schakra2}@binghamton.edu

***Abstract*—We analyze a class of first significant digit (FSD) histogram restoration techniques designed to cover up traces of previous JPEG compressions under a minimum cost constraint. We argue that such minimal distortion mappings introduce strong artifacts to the distribution of DCT coefficients, which become particularly prevalent in the domain of second significant digits (SSDs). Empirical findings from large image databases give insight into SSD distributions of DCT coefficients of natural images and demonstrate how images that underwent FSD histogram restoration deviate from natural images.**

I. Introduction

Over the past decade, image forensics has matured to become a research field where advances are critically assessed under a security perspective more routinely. Embedded into the broader trend of adversarial signal processing [1], counter-forensics [2] subsumes attempts to systematically mislead forensic techniques. While early works were mostly of heuristic nature [3], there is now a growing body of theoretical works that contribute to the necessary rigorous foundations [4], [5].

Driven by the widespread use of JPEG images, the compression history of digital images is among the most extensively studied subjects. A standard problem on the forensic side is the detection of previous JPEG compressions. Also counter-forensic methods to make JPEG images look like uncompressed ones or to hide traces of double compression abound [6], [7]. These developments have led to a new generation of forensic algorithms focusing on traces left by counter-forensics [8], [9].

This paper follows the fruitful path of interaction between forensics and counter-forensics. Our particular emphasis is on a recent class of counter-forensic techniques that restore first significant digit (FSD) histograms of block-DCT coefficients to cover up artifacts of previous JPEG compression(s) under a minimum distortion constraint [10], [11]. We demonstrate how optimal FSD histogram restoration has a strong impact on the distribution of second significant digits (SSDs), which may be exploited to detect FSD restoration. Along the way, we provide insights into SSD distributions of block-DCT modes of natural images, which appear to follow a Benford-like law in certain instances.

In the remainder of this paper, Sect. II briefly reviews the current literature on FSD forensics and counter-forensics, before Sect. III discusses how SSDs of FSD-restored sequences differ from natural sequences. Sect. IV introduces some theoretical background on SSD distributions. Sect. V describes our experimental setup to explore empirical aspects of SSD distributions and histogram restoration in Sects. VI and VII. Sect. VIII concludes the paper.

II. FSD Image Forensics and Counter-Forensics

A. First Significant Digits and Benford's Law

We follow the notation in [11] and write the first significant digit (FSD) of a non-zero number $x \in \mathbb{R} \setminus \{0\}$ as

$$\mathsf{d}_1(x) = \left\lfloor \frac{|x|}{10^{\lfloor \log_{10} |x| \rfloor}} \right\rfloor = \left\lfloor 10^{\mathsf{c}(x)} \right\rfloor , \tag{1}$$

where $\mathsf{c}(x) = \log_{10}|x| - \lfloor \log_{10}|x| \rfloor = \log_{10}|x| \mod 1$ is the coset representative of x in Benford's domain. With bin boundaries

$$b_i = \log_{10}(i+1) , \tag{2}$$

the i-th FSD histogram bin of a sequence $\boldsymbol{x} = (x_1, \ldots, x_N)$, $x_k \neq 0$, is given as

$$\mathsf{h}_1(\boldsymbol{x}, i) = \big|\{x_k : b_{i-1} \leq \mathsf{c}(x_k) < b_i\}\big| , \; 1 \leq i \leq 9 . \tag{3}$$

The FSD histogram of $\boldsymbol{x}$ is $\mathsf{h}_1(\boldsymbol{x}) = (\mathsf{h}_1(\boldsymbol{x}, 1), \ldots, \mathsf{h}_1(\boldsymbol{x}, 9))$. A sequence $\boldsymbol{x}$ is said to follow Benford's law [12] if

$$\mathsf{h}_1(\boldsymbol{x}, i) \approx N \log_{10}(1 + 1/i) . \tag{4}$$

A sufficient condition for Benford's law to be satisfied is a uniform distribution of $\mathsf{c}(x)$ over the interval $[0, 1)$ [13].

It is commonly assumed that block-DCT modes of natural images obey Benford's law to some degree (amongst many other types of "natural" data), yet generalized forms of the law have also been proposed to be more compliant with empirical FSD distributions of DCT coefficients from uncompressed images [14] or quantized JPEG coefficients [15].

B. Image Forensics Based on First Significant Digits

A number of forensic techniques work with assumptions about the distribution of first significant digits of block-DCT coefficients. Inference about the JPEG compression history of digital images is a typical application, for instance to determine whether a bitmap image had been JPEG compressed before, or whether a JPEG image underwent multiple compression cycles. The common working assumption of these methods is that lossy JPEG compression changes the FSD distribution

of an image's DCT coefficients. Early approaches explored a relatively straightforward adoption of Benford's law, attempting to verify whether or not quantized JPEG coefficients are well-behaved in the Benford sense [15], [16]. More recent techniques put a stronger emphasis on machine learning support [17]. FSD-based approaches are generally among the most powerful methods for analyzing the compression history of digital images, in particular when multiple JPEG compressions are concerned [17].

C. First Significant Digit Histogram Restoration

Promising results of FSD forensics have recently sparked interest in counter-forensic approaches that attempt to restore FSD statistics of processed images [10], [11], [18], [19]. In this work, we are particularly interested in the class of algorithms that operate under a distortion constraint, i. e., given a (possibly processed) *source* sequence $\boldsymbol{x}$, the goal is to find a sequence $\boldsymbol{x}^*$ of the same length as $\boldsymbol{x}$ that adheres to a desired *target* FSD distribution $\boldsymbol{h}^*$ while being as similar as possible to the source. Distortion is measured in terms of a suitable cost function $\mathsf{g} : \mathbb{R}^N \times \mathbb{R}^N \to \mathbb{R}$. More formally,

$$\boldsymbol{x}^* = \arg \min_{\tilde{\boldsymbol{x}}:\mathsf{h}_1(\tilde{\boldsymbol{x}})=\boldsymbol{h}^*} \mathsf{g}(\boldsymbol{x}, \tilde{\boldsymbol{x}})\,. \tag{5}$$

The literature has pointed out that solving Eq. (5) for individual block-DCT modes under a mean squared error (MSE) distortion regime is equivalent to minimizing the spatial domain MSE distortion incurred by DCT-domain FSD histogram restoration [10], [11]. We further note that more general optimization scenarios may also involve an additional minimization over a set of admissible target histograms [4], [11].

Solutions to Eq. (5) have been found by reformulating the problem in terms of transportation theory [10] or linear optimization [11]. Both approaches exploit that MSE distortion is component-wise additive and consider a cost matrix $\boldsymbol{M}$ of dimension $9 \times N$. The (i,k)-th entry of $\boldsymbol{M}$ holds the minimum element-wise cost of mapping x_k to a value $\mathsf{m}(x_k, i)$ with $\mathsf{d}_1(\mathsf{m}(x_k, i)) = i$. The costs depend on the set of candidate values that x_k can be mapped to. In the following, we will assume $\mathsf{m} : \mathbb{R} \to \mathbb{Z} \cdot 10^{-p}$ for some numeric precision $p \geq 0$,

$$\mathsf{m}(x_k, i) = \arg\min_{\substack{\tilde{x}\in\mathbb{Z}\cdot 10^{-p} \\ \mathsf{d}_1(\tilde{x})=i}} (x_k - \tilde{x})^2 \tag{6}$$

$$M_{i,k} = (x_k - \mathsf{m}(x_k, i))^2\,. \tag{7}$$

Defining a permutation σ with $|x_{\sigma(k)}| \geq |x_{\sigma(k)-1}|$, Pasquini et al. [10] iterate over column indices $\sigma(k)$ and obtain $x^*_{\sigma(k)}$ with FSD i^* as

$$i^* = \arg\min_{i\,:\,h_i^*>0} M_{i,\sigma(k)}\,, \tag{8}$$

$$x^*_{\sigma(k)} = \mathsf{m}(x_{\sigma(k)}, i^*)\,, \tag{9}$$

decreasing the i^*-th element of the target histogram $\boldsymbol{h}^*$ by one after each iteration. While this heuristic procedure solves the transportation-theoretic formulation of Eq. (5) only suboptimally [10], it does ensure that elements with large magnitudes remain largely undistorted, yielding a relatively low overall distortion.

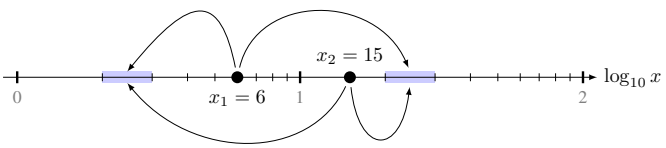

Fig. 1. FSD mapping candidate intervals for two values $x_1 = 6$ and $x_2 = 15$, depicted on a logarithmic scale, when mapping to a first significant digit of 2. The highlighted intervals correspond to coset representatives $b_1 \leq \mathsf{c}(\tilde{x}) < b_2$, i. .e, $\mathsf{d}_1(\tilde{x}) = 2$.

Comesaña and Pérez-González [11] find the global minimum distortion mapping by solving

$$\min_{A_{i,k}\in\{0,1\}} \sum_{i=1}^{9}\sum_{k=1}^{N} A_{i,k} \cdot M_{i,k}\,, \tag{10}$$

subject to the constraints $\sum_{i=1}^{9} A_{i,k} = 1$ and $\sum_{k=1}^{N} A_{i,k} = h_i^*$. The simplex algorithm yields a solution to this standard linear optimization problem. Comesaña and Pérez-González also point out that the nature of the optimization problem guarantees a solution with binary coefficients $A_{i,k}$, i. e., a sequence with elements

$$x_k^* = \mathsf{m}(x_k, \arg\max_i A_{i,k}) \tag{11}$$

will have an FSD histogram equal to the target histogram $\boldsymbol{h}^*$. Experimental results in [11] indicate that the simplex solution is indeed superior to prior heuristic approaches.

III. Histogram Restoration Artifacts

A closer examination of Eq. (6) highlights that finding the optimal x^* with a desired first significant digit $\mathsf{d}_1(x^*) = i$ entails evaluating at most two values [11]. Candidate mappings of source values x with $\mathsf{d}_1(x) \neq i$ may be found in the coset intervals $b_{i-1} \leq \mathsf{c}(\tilde{x}) < b_i$ left or right of x, cf. Fig. 1. To the right, the number closest to $\log_{10}|x|$ is

$$\begin{aligned}\mathsf{r}(x,i) &= b_{i-1} + \lceil \log_{10}|x| - b_{i-1} \rceil \\ &= b_{i-1} + \begin{cases} \lfloor \log_{10}|x| \rfloor + 1 & \text{if } \mathsf{d}_1(x) > i \\ \lfloor \log_{10}|x| \rfloor & \text{if } \mathsf{d}_1(x) < i\,. \end{cases}\end{aligned} \tag{12}$$

The supremum of the left interval is

$$\begin{aligned}\mathsf{l}(x,i) &= b_i \quad + \lfloor \log_{10}|x| - b_i \rfloor \\ &= b_i \quad + \begin{cases} \lfloor \log_{10}|x| \rfloor & \text{if } \mathsf{d}_1(x) > i \\ \lfloor \log_{10}|x| \rfloor - 1 & \text{if } \mathsf{d}_1(x) < i\,. \end{cases}\end{aligned} \tag{13}$$

The corresponding candidate values are

$$\mathsf{r}^*(x,i) = \quad \operatorname{sgn}(x) \cdot 10^{\mathsf{r}(x,i)} \tag{14}$$

$$\mathsf{l}^*(x,i) = \begin{cases} \operatorname{sgn}(x)\,\left(10^{\mathsf{l}(x,i)} - 10^{-p}\right) & \text{if } \mathsf{l}(x,i) \geq -p \\ -\infty & \text{else,} \end{cases} \tag{15}$$

and the mapping returns

$$\mathsf{m}(x,i) = \begin{cases} x & \text{if } \mathsf{d}_1(x) = i \\ \arg\min\limits_{n\in\left\{\substack{\mathsf{r}^*(x,i) \\ \mathsf{l}^*(x,i)}\right\}} (x-n)^2 & \text{else.} \end{cases} \tag{16}$$

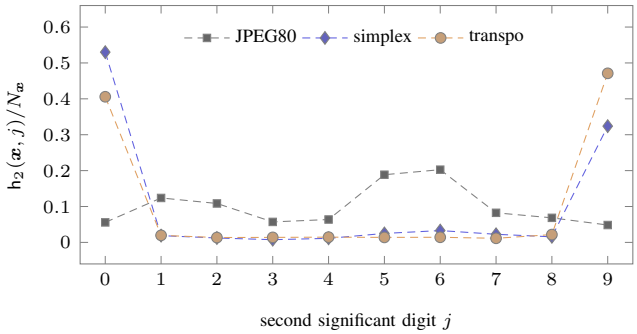

Fig. 2. SSD histogram of the $(5,0)$-th DCT coefficient before and after transportation-theoretic and simplex FSD histogram restoration. Target histogram: Benford's law; $p=6$; source image: `ucid00505`, JPEG QF 80.

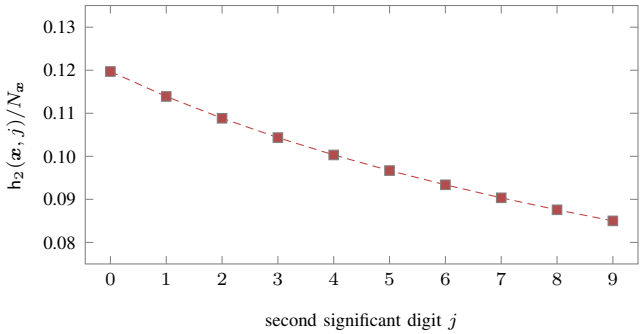

Fig. 3. Distribution of second significant digits according to Benford's law.

We note that Comesaña and Pérez-González [11] were only interested in determining the optimal costs and thus worked with the supremum $\mathsf{I}(x,i)$ instead of $\mathsf{I}^*(x,i)$. Practical histogram restoration has to take finite precision effects into account. This implies that, if an element x_k needs to be modified to adjust the FSD histogram of sequence $\boldsymbol{x}$, the mapping $\mathsf{m}(x_k,i)$ will have a *second significant digit* equal to zero (Eq. (14)) or nine (Eq. (15)). Setting $p=3$ in the example in Fig. 1 for instance, $x_1=6$ would be mapped to 2.999, $x_2=15$ would be mapped to 20. This effect will be observable unless $\mathsf{m}(x_k,i)=i10^{-p}$ (e. g., $\mathsf{m}(6,2)=2$ for $p=0$).

Figure 2 gives an illustrative example for a randomly chosen image from the UCID image database, stored as JPEG with quality factor 80.[1] The graphs depict the relative frequencies of second significant digits of the $(5,0)$-th DCT coefficient, before and after FSD histogram restoration based on Eqs. (9) and (11). The FSD target histogram was set to comply with Benford's law, cf. Eq. (4). Histogram restoration artifacts are clearly visible from the graphs, which indicate a strong increase of second significant digits zero and nine.

IV. Second Significant Digit Statistics

The second significant digit (SSD) of a non-zero number $x\in\mathbb{R}\setminus\{0\}$ is commonly defined in accordance to the notion of first significant digits,

$$\mathsf{d}_2(x)=\lfloor 10^{\mathsf{c}(x)+1}\rfloor-10\lfloor 10^{\mathsf{c}(x)}\rfloor\,. \tag{17}$$

Different from FSDs, $\mathsf{d}_2(x)\in\{0,\ldots,9\}$ may also equal zero (see also Fig. 2). The SSD histogram of a sequence $\boldsymbol{x}$, $\mathsf{h}_2(\boldsymbol{x})=(\mathsf{h}_2(\boldsymbol{x},0),\ldots,\mathsf{h}_2(\boldsymbol{x},9))$, follows the logic of Eq. (3), so we omit an explicit definition. Note that Eq. (17) does not differentiate between significant digits and trailing zeros of finite precision numbers, i. e., $\mathsf{d}_2(9)=0$. For the sake of simplicity, we still use the above notation to refer to SSDs, but ignore the set $\{x:x=\mathsf{d}_1(x)\}$ when compiling SSD histograms. This implies that the number of elements of a non-zero sequence $\boldsymbol{x}$ that contribute to aggregate statistics may vary. We use symbol $N_{\boldsymbol{x}}$ to count the number of elements with a well-defined SSD.

Although Benford's law is often associated with properties of FSD distributions only, a uniform distribution of $\mathsf{c}(x)$ over $[0,1)$ clearly has implications on the joint distribution of *all* decimal digits. Denoting $\Pr(D_s=d_s)$ as the probability that the s-th significant digit equals d_s, an extended variant of Benford law states that [13]

$$\Pr\big((D_1,D_2,\ldots,D_r)=(d_1,d_2,\ldots,d_r)\big)=\log_{10}\Big(1+\big(\textstyle\sum_{s=1}^{r}10^{s-r}d_s\big)^{-1}\Big)\,. \tag{18}$$

It follows directly from Eq. (18) that a sequence $\boldsymbol{x}$ compliant with Benford's law should satisfy

$$\mathsf{h}_2(\boldsymbol{x},j)\approx N_{\boldsymbol{x}}\sum_{i=1}^{9}\log_{10}\left(1+\frac{1}{10i+j}\right)\,. \tag{19}$$

Figure 3 presents a graphical representation of Eq. (19) and depicts the ideal SSD distribution according to Benford's law. Observe that the distribution is much more uniform than the FSD distribution. Generally speaking, Benford's law implies that the distribution of the s-th digit approaches the uniform distribution as $s\to\infty$ [20].

V. Experimental Setup

Before we continue with a more detailed empirical exposition of SSD distribution characteristics of DCT coefficients, we give a brief overview of our experimental setup. Experimental results are based on the UCID [21] and the RAISE-2k [22] image databases. The UCID dataset comprises 1338 uncompressed images of size 384×512, very likely downscaled from larger digital camera images. The RAISE-2k dataset is a subset of the RAISE database. It contains 2000 uncompressed full-resolution images from three different digital cameras, with resolutions ranging from 6 to 15 megapixels. All images were converted to grayscale before any processing.[2] We used the Independent JPEG Group reference library with floating-point DCT implementation and standard quantization tables to obtain JPEG versions of the databases. DCT coefficients, rounded to 6 digits before analysis, were computed from non-overlapping 8×8 pixel blocks with integer intensities in the range $[0,255]$ after subtracting a constant offset of 128. The blocks were aligned with the JPEG grid, if the image was previously stored as JPEG. Simplex problems were solved with the lpSolve package for R[3], with the scale parameter set to 1000.

[1] We refer to Sect. V for a description of our databases and processing steps.

[2] ImageMagick `convert` with option `-grayscale Rec601Luma`.

[3] http://cran.r-project.org/web/packages/lpSolve

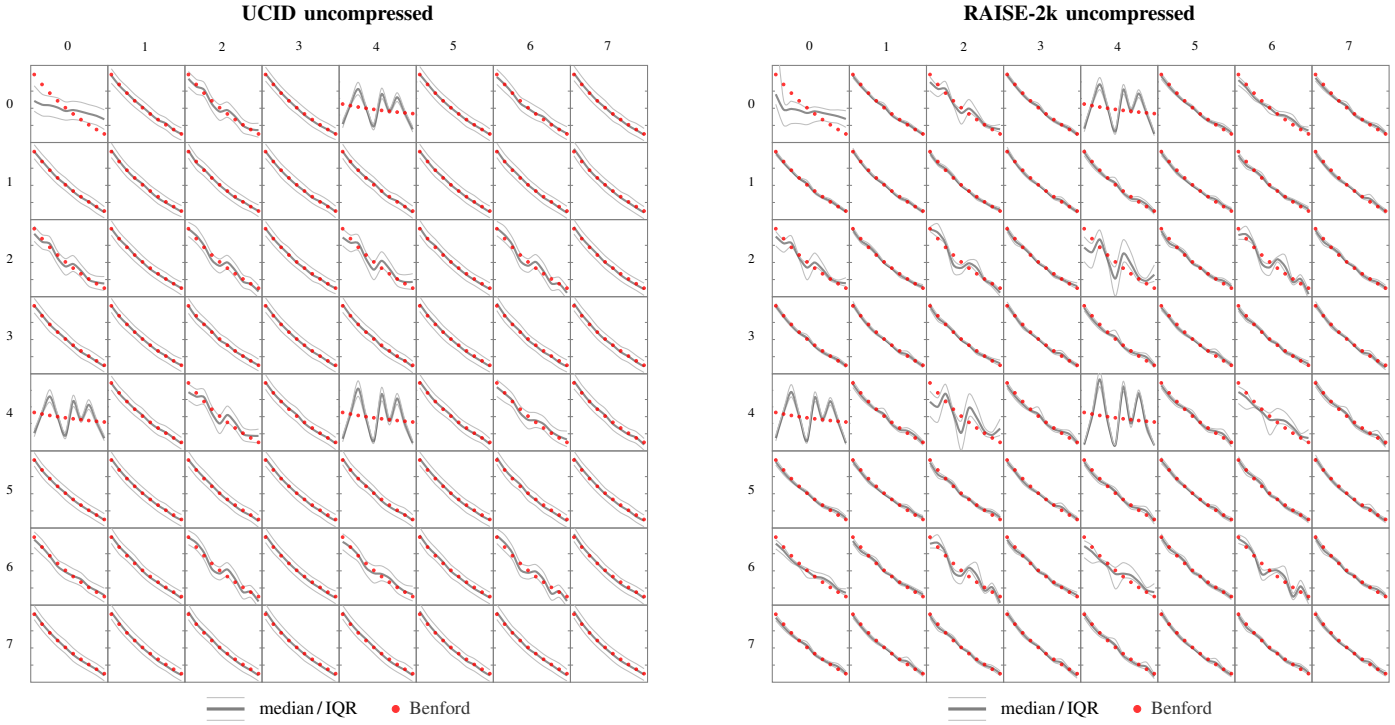

Fig. 4. Empirical SSD distributions of 8×8 block-DCT coefficients from the UCID (left) and the RAISE-2k (right) image database. Subfigures are arranged in correspondence with DCT mode indices and depict the medians, the 25 % quartiles and the 75 % quartiles of relative frequencies for digits $\{0, \ldots, 9\}$ (from left to right within each subfigure). Red circles denote the distribution predicted by Benford's law (equal for all coefficients). All subfigures are plotted on the same vertical scale, except for coefficients $(4, 0)$, $(0, 4)$ and $(4, 4)$.

VI. Second Significant Digits in the DCT Domain

Several works in the literature have reported that first significant digits of block-DCT coefficients obey Benford's law (or a generalized variant) strikingly well [14], [15]. Distributions of other digits were not in the focus of these works. Figure 4 sheds some light on this aspect and will help to understand the impact of FSD restoration in the DCT domain. For each of the 8×8 DCT coefficient indices, the figure depicts the medians, the 25 % quartiles and the 75 % quartiles of relative SSD frequencies obtained from the UCID (left panel) and the RAISE-2k (right panel) database. Each subfigure contains a reference graph of the SSD distribution according to Benford's law (see also Fig. 3).

Our measurements suggest that most of the DCT modes are in good alignment with Eq. (19). Particularly notable deviations exist for the DC mode $(0, 0)$, and for coefficients $(0, 4)$, $(4, 0)$ and $(4, 4)$. An analytical justification is beyond the scope of this manuscript, but we suspect that this can be explained from the particular form of the DCT transformation matrix, which is constant (up to sign alternations) in the 0-th and in the 4-th row.[4] Indications of further deviations for DCT coefficients with even row or column indices in the UCID database are more pronounced in the much larger RAISE-2k image set. Also here, an inspection of the DCT transformation matrix reveals that rows with even indices are composed of two different transform coefficients only (again, up to sign alternations) and thus differ fundamentally from odd matrix rows.

[4]Denoting $\boldsymbol{D}$ the DCT transformation matrix, the DCT of a 2D signal $\boldsymbol{Y}$ can be written as $\boldsymbol{X} = \boldsymbol{D}\boldsymbol{Y}\boldsymbol{D}^\top$.

VII. Exposing FSD Histogram Restoration

Our findings in the previous section clearly indicate that SSD distributions of 8×8 block-DCT coefficients from natural images follow certain regularities. Similar to FSD distributions, Benford's law seems to be a suitable model, at least for DCT coefficients with odd row and column indices. Other coefficients show a more complex, yet still relatively consistent behavior, even across substantially different image sets. Considering that FSD histogram restoration may leave strong artifacts in the SSD histogram of a restored DCT coefficient sequence (cf. Sect. III), we now ask how well images that underwent histogram restoration are distinguishable from unprocessed ones.

For an experimental examination, we JPEG-compressed all UCID images with quality factors in $\{30, 35, 40, \ldots, 100\}$. Non-zero DCT coefficients of the JPEG compressed images, obtained from the images' spatial domain representations, were then modified using the restoration techniques based on Eqs. (9) and (11). The target histograms were set to achieve FSD distributions compliant with Benford's law. We restored each individual coefficient index individually with precision $p = 6$. The DC coefficient always remained unmodified, in accordance with the literature.

Figure 5 exemplarily illustrates the SSD distributions resulting from simplex restoration [11] of JPEG source images with quality factors 50 and 90. For each of the 63 restored DCT coefficient indices, the figure depicts the median relative SSD frequencies, aggregated over all images in the UCID database. Each subfigure contains a reference graph of the theoretical Benford distribution (see also Fig. 3). The left panel of Fig. 5 corresponds to the "ideal" scenario, where DCT coefficients

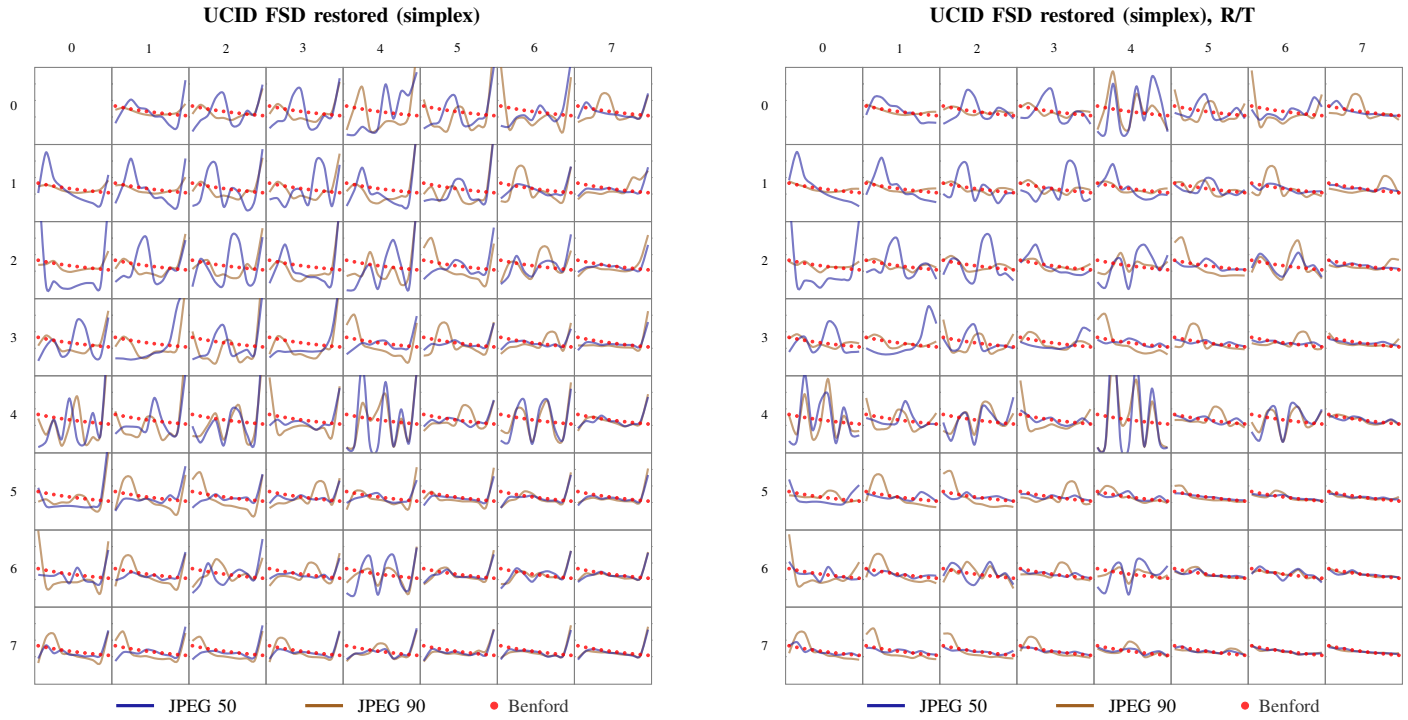

Fig. 5. Empirical SSD distributions of 8×8 block-DCT coefficients from the UCID image database (JPEG compressed with quality factors 50 and 90) after simplex FSD histogram restoration ($p = 6$, target histograms: Benford's law, DC coefficient unmodified). Left: ideal restoration; right: after inverse DCT and spatial domain rounding/truncation (R/T) to integer intensities. Subfigures are arranged in correspondence with DCT mode indices and depict the medians of relative frequencies for digits $\{0, \ldots, 9\}$ (from left to right within each subfigure). Red circles denote the SSD distribution predicted by Benford's law (equal for all coefficients). All subfigures are plotted on the same vertical scale.

are analyzed immediately after FSD histogram restoration. The right panel includes an additional rounding/truncation (R/T) step in the spatial domain, mimicking the effect of saving the restored image in an uncompressed image format before analysis. It can be expected that FSD restoration effects (both in terms of the FSD and the SSD histograms) will be attenuated in this more realistic scenario.

A direct comparison of Figs. 4 and 5 clearly reveals how substantially FSD-restored images differ from uncompressed natural images. None of the DCT coefficients in the left panel is even close to Benford's distribution of second significant digits. After restoration, most coefficients have a strong bias towards digits zero and/or nine. This effect is less pronounced after the R/T step, especially in the high-frequency modes. Nevertheless, strong irregularities prevail throughout the mid and low-frequency bands, depending on the quality factor of the source image.

Quantitatively, these apparent differences can be measured, for instance, in terms of the χ^2 divergence between the empirical relative frequencies and Benford's distribution,

$$\chi^2 = \sum_{j=0}^{9} \frac{\left(\mathrm{h}_2(\boldsymbol{x}, j)/N_{\boldsymbol{x}} - \sum_{i=1}^{9} \log_{10}\left(1 + \frac{1}{10i+j}\right)\right)^2}{\sum_{i=1}^{9} \log_{10}\left(1 + \frac{1}{10i+j}\right)} \quad (20)$$

which we evaluate individually for each DCT coefficient index $(2m+1, 2n+1)$, $0 \leq m, n \leq 3$. This selection of coefficients is inspired by our observations in Sect. VI. Figure 6 summarizes our results for a scenario where the average χ^2 over the selected indices would be used as a decision criterion to detect FSD-restored images. The graphs depict the minimum and maximum averaged χ^2 after restoration with R/T as a function of the source image's JPEG quality factor. The maximum averaged χ^2 from the set of all original uncompressed images is shown as a horizontal detection threshold. Observe that we achieve a perfect separation for both restoration techniques throughout all 15 tested JPEG quality factors. Note that we only display graphs for the more realistic R/T scenario. We observed an even stronger separation when FSD-restored images are analyzed directly. We also point out that more sophisticated detectors may exploit higher-dimensional SSD-based features to strive for a stronger separation when the restoration of high-quality JPEGs is concerned.

VIII. Concluding Remarks

We have studied artifacts of state-of-the-art first significant digit (FSD) histogram restoration techniques [10], [11]. These algorithms map source histograms to desired target histograms while attempting to minimize the distortion with respect to the source sequence. A typical application is the restoration of block-DCT coefficient FSD histograms of JPEG compressed images to a Benford-like distribution, such that the modified image appears like an uncompressed image to forensic detectors. We have argued that such mappings under a minimal distortion constraint have a strong impact on the distribution of second significant digits (SSD). Backed with empirical evidence from large image databases, our results indicate that FSD-restored images exhibit SSD distributions that differ substantially from those of uncompressed natural images. An extension of this analysis to the restoration of (quantized) JPEG coefficients is

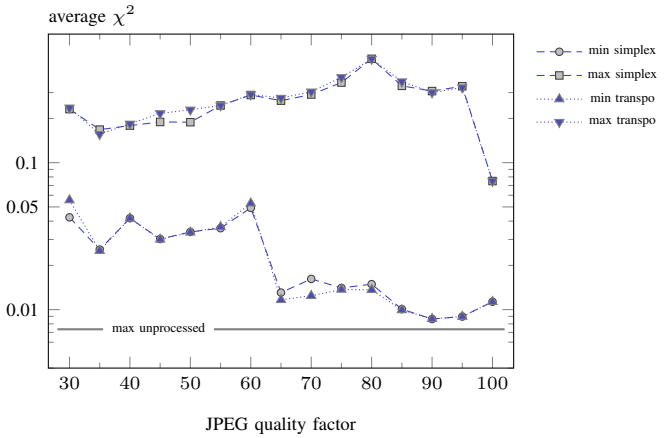

Fig. 6. Averaged χ^2 divergence between empirical SSD distributions and Benford's law after FSD histogram restoration and spatial domain R/T; average computed over odd-indexed DCT coefficients. The graphs show the minimum and maximum divergences of all JPEG-compressed UCID images after FSD histogram restoration. The horizontal line corresponds to the maximum averaged χ^2 in the set of all original uncompressed images.

subject to future work. Future work will also have to show whether existing FSD histogram restoration techniques can be augmented to cover up SSD artifacts—thus entering the next iteration in the the cat-and-mouse game between forensics and counter-forensics [2]. Potential approaches may include a randomized (but sub-optimal, in the FSD-sense) mapping function, or a largely extended set of constraints to the linear optimization formulation of the FSD histogram restoration problem. In view of the ever-increasing toolbox of JPEG forensics [23], we remain reserved on whether restoring a single statistical characteristic will ever suffice to fool forensic investigators, however.

On a more general level, this manuscript is—to the best of our knowledge—the first work that studies significant digit distributions of block-DCT coefficients beyond the FSD. Our results from the UCID and the RAISE-2k image sets indicate that second significant digits of certain DCT modes have a Benford-like behavior. DCT coefficients with even row or column indices differ more substantially, but show a relatively consistent behavior across different images. Further investigations will show how these findings may contribute to a deepened understanding of DCT coefficient FSD distributions, and whether forensic applications beyond the one discussed in this manuscript exist. In particular, it will be interesting to see how (multiple) JPEG compression(s) and image processing affect second significant digits of DCT/JPEG coefficients.

Acknowledgments

The authors thank Cecilia Pasquini and Pedro Comensaña for providing reference implementations of their histogram restoration algorithms.

References

[1] M. Barni and F. Pérez-González, "Coping with the enemy: Advances in adversary-aware signal processing," in *IEEE International Conference on Acoustics, Speech and Signal Processing*, 2013, pp. 8682–8686.

[2] R. Böhme and M. Kirchner, "Counter-forensics: Attacking image forensics," in *Digital Image Forensics: There is More to a Picture Than Meets the Eye*, H. T. Sencar and N. Memon, Eds. Springer-Verlag, 2013, pp. 327–366.

[3] M. Kirchner and R. Böhme, "Hiding traces of resampling in digital images," *IEEE Transactions on Information Forensics and Security*, vol. 3, no. 4, pp. 582–592, 2008.

[4] P. Comesaña and F. Pérez-González, "Optimal counterforensics for histogram-based forensics," in *IEEE International Conference on Acoustics, Speech and Signal Processing*, 2013, pp. 3048–3052.

[5] M. Barni and B. Tondi, "The source identification game: An information-theoretic perspective," *IEEE Transactions on Information Forensics and Security*, vol. 8, no. 3, pp. 450–463, 2013.

[6] M. C. Stamm and K. J. R. Liu, "Anti-forensics of digital image compression," *IEEE Transactions on Information Forensics and Security*, vol. 6, no. 3, pp. 1050–1065, 2011.

[7] W. Fan, K. Wang, F. Cayre, and Z. Xiong, "A variational approach to JPEG anti-forensics," in *IEEE International Conference on Acoustics, Speech, and Signal Processing*, 2013, pp. 3058–3062.

[8] S. Lai and R. Böhme, "Countering counter-forensics: The case of JPEG compression," in *Information Hiding, 13th International Conference*, ser. Lecture Notes in Computer Science, T. Filler, T. Pevný, S. Craver, and A. Ker, Eds., vol. 6958. Springer Verlag, 2011, pp. 285–298.

[9] G. Valenzise, M. Tagliasacchi, and S. Tubaro, "Revealing the traces of JPEG compression anti-forensics," *IEEE Transactions on Information Forensics and Security*, vol. 8, no. 2, pp. 335–349, 2013.

[10] C. Pasquini, P. Comesaña, F. Pérez-González, and G. Boato, "Transportation-theoretic image counterforensics to first siginificant digit histogram forensics," in *IEEE International Conference on Acoustics, Speech and Signal Processing*, 2014, pp. 2699–2703.

[11] P. Comesaña and F. Pérez-González, "The optimal attack to histogram-based forensic detectors is simple(x)," in *IEEE International Workshop on Information Forensics and Security*, 2014, pp. 1730–1735.

[12] F. Benford, "The law of anomalous numbers," *Proceedings of the American Philosophical Society*, vol. 78, no. 4, pp. 551–572, 1938.

[13] A. Berger, "A basic theory of Benford's law," *Probability Surveys*, vol. 8, pp. 1–126, 2011.

[14] F. Pérez-González, G. L. Heileman, and C. T. Abdallah, "Benford's law in image processing," in *IEEE International Conference on Image Processing*, vol. 1, 2007, pp. 405–408.

[15] D. Fu, Y. Q. Shi, and W. Su, "A generalized Benford's law for JPEG coefficients and its applications in image forensics," in *Security and Watermarking of Multimedia Content IX*, ser. Proceedings of SPIE, E. J. Delp and P. W. Wong, Eds., vol. 6505, 2007, 65051L.

[16] B. Li, Y. Q. Shi, and J. Huang, "Detecting doubly compressed JPEG images by using mode based first digit features," in *IEEE Workshop on Multimedia Signal Processing*, 2008, pp. 730–735.

[17] S. Milani, M. Tagliasacchi, and S. Tubaro, "Discriminating multiple JPEG compressions using first digit features," *APSIPA Transactions on Signal and Information Processing*, vol. 3, e19, 2014.

[18] ——, "Antiforensics attacks to Benford's law for the detection of double compressed images," in *IEEE International Conference on Acoustics, Speech and Signal Processing*, 2013, pp. 3053–3057.

[19] C. Pasquini and G. Boato, "JPEG compression anti-forensics based on first significant digit distribution," in *IEEE Workshop on Multimedia Signal Processing*, 2013, pp. 500–505.

[20] P. Diaconis, "The distribution of leading digits and uniform distribution mod 1," *The Annals of Probability*, vol. 5, no. 1, pp. 72–81, 1977.

[21] G. Schaefer and M. Stich, "UCID – an uncompressed colour image database," in *Storage and Retrieval Methods and Applications for Multimedia*, ser. Proceedings of SPIE, M. M. Yeung, R. W. Lienhart, and C.-S. Li, Eds., vol. 5307, 2004, pp. 472–480.

[22] D.-T. Dang-Nguyen, C. Pasquini, V. Conotter, and G. Boato, "RAISE: a raw images dataset for digital image forensics," in *6th ACM Multimedia Systems Conference*, 2015, pp. 219–224.

[23] J. Yang, G. Zhu, J. Huang, and X. Zhao, "Estimating JPEG compression history of bitmaps based on factor histogram," *Digital Signal Processing*, vol. 41, pp. 90–97, 2015.